5226 *Macromolecules* **2009**, *42*, 5226–5235
DOI: 10.1021/ma900361p

Macromolecules
ARTICLE

SDS Interactions with Hydrophobically End-Capped Poly(ethylene oxide) Studied by ^{13}C NMR and SANS

Chantal Rufier,[†,‡] André Collet,[†] Michel Viguier,*[,†] Julian Oberdisse,[§,⊥] and Serge Mora[§]

[†]*Institut Charles Gerhardt UMR-CNRS 5253 and* [§]*Laboratoire des Colloïdes, Verres et Nanomatériaux, UMR-CNRS 5587, Université Montpellier 2, C.C 1702, Pl. E. Bataillon F-34095 Montpellier Cedex 05, France, and* [⊥]*CEA Saclay, Laboratoire Leon Brillouin, F-91191 Gif Sur Yvette, France.* [‡] *Present address: Adolphe Merkle Institute, Ilford Bat. 180, Route de l'Ancienne Papeterie, CH 1723 Marly, Switzerland*

Received February 17, 2009; Revised Manuscript Received May 4, 2009

ABSTRACT: The interactions, in aqueous medium, between hydrophobically end-capped poly(ethylene oxide) (PEO) and sodium dodecyl sulfate (SDS) have been investigated by means of tensiometry, ^{13}C NMR spectroscopy and small-angle neutron scattering (SANS). Besides the association of SDS with the ethylene oxide backbone of associative polymer (AP), revealed by ^{13}C NMR, SDS interacts with hydrophobic end-caps leading to the formation of mixed aggregates. At low SDS concentration, the formation of flowerlike mixed aggregates is governed by AP. Despite the poor affinity between hydrocarbon and fluorocarbon chains, uncooperative binding was detected between SDS and fluorinated AP end groups. With a further increase of SDS concentration, the critical aggregation concentration (cac) marks the onset of SDS cooperative binding with AP end-caps. This process driven by SDS leads to the formation of micellar aggregates with a necklacelike structure. Due to the SDS/AP complex formation, the surfactant aggregation number determined by SANS is lower than that observed in pure water.

1. Introduction

Associative polymers (APs) are used in a wide range of applications as viscosifying agents and rheology modifiers of aqueous systems.[1] According to the hydrophobic/hydrophilic balance, these amphiphilic polymers can present a phase segregation in aqueous medium with a dilute solution of polymer and a viscous gellike phase. The phase separation is enhanced by the presence of highly hydrophobic perfluorinated groups. This phenomenon, explained by the theory developed by Semenov et al.,[2] was more easily investigated using telechelic APs that can be considered as model polymers. It was established, with fully hydrophobically end-capped poly(ethylene oxide) (PEO M_n = 20000 g/mol), that phase separation occurs when the length of the hydrophobic end group exceeds 18 CH_2 (or the equivalent CH_2).[3] Addition of surfactant improves homogenization of the ternary system. A very small amount of surfactant is sufficient to prevent phase separation. For instance it was found that the ternary system SDS/$C_8F_{17}(CH_2)_{10}$-PEO20k-$(CH_2)_{10}C_8F_{17}$/water is homogeneous when the molar ratio C_{SDS}/C_{pol} is equal to 0.3, whatever the AP concentration (C_{pol}).[3] The role of surfactant is not limited to the homogenization of ternary mixtures, the rheological properties are also profoundly modified. Upon addition of surfactant to a solution of AP, the viscosity increases, passes through a maximum for a surfactant concentration close to its critical micelle concentration (cmc) in pure water solution, and then decreases.[4−6] Similar trends are observed with the plateau modulus (G_0) at low polymer concentration and with the viscoelastic relaxation time (τ).[7] The rheological response in presence of anionic surfactant is complex due to the interactions of surfactant with hydrophobic end groups of AP (as observed with mixtures of surfactants) but also with the PEO hydrophilic chain. Interactions of SDS with PEO have been investigated by several authors involving various techniques such as tensiometry,[8] microcalorimetry,[9−12] conductimetry,[13,14] light[15] and neutron[16] scattering, fluorescence spectroscopy,[17,18] NMR spectroscopy,[11,14] or ESR.[19−21] Interactions between SDS and PEO depend on surfactant concentration and PEO molecular weight. Increasing SDS concentration in PEO solutions generates two transition points. The critical aggregation concentration (cac) corresponds to the onset of cooperative binding of SDS micelles with the PEO chain. The cac occurs in a lower range of SDS concentrations (between 4 and 5 mM) than the corresponding cmc (8 mM). The SDS micelles complexed by PEO chain are smaller than in pure water with an aggregation number of about 20 monomer units versus 60 without PEO.[17] The second transition point, sometimes called polymer saturation point (psp), is observed when the SDS concentration exceeds the critical concentration C_m corresponding to saturation of polymer chain and formation of free SDS micelles. As a consequence C_m increases with PEO concentration in the solution. The PEO molecular weight has little or no effect on solution properties when it is greater than 4000 g/mol,[11] meaning that the stabilization of SDS micelles by the PEO chain needs about 100 ethylene oxide monomer units. Otherwise micellar properties of cationic surfactants such as dodecyltrimethylammonium bromide or tetradecyltrimethylammonium bromide are not affected by the presence of PEO[12,17] indicating that only anionic surfactants interact significantly with PEO.

The binding interactions between SDS and hydrophobically modified PEO are more complex. In addition to the cooperative interactions of SDS with the PEO chain, uncooperative hydrophobic binding interactions are also present. The uncooperative binding process results in very small enthalpy changes which are not detectable by isothermal titration calorimetric (ITC).[22] From rheological results[7] and fluorescence studies,[23] it was suggested that the association of SDS molecules with the AP hydrophobic end groups with formation of mixed micelles starts at low SDS concentrations, well below the cmc of SDS itself. From light

*To whom correspondence should be addressed. E-mail: michel.viguier@univ-montp2.fr. Telephone: 33-467 14 32 13. Fax: 33-467 14 40 28.

 Published on Web 06/25/2009

scattering results,[24] an average aggregation number of about 20 was estimated for the flowerlike mixed aggregates. Most of these studies were performed with pyrene end-capped PEO[23,25] or hydrophobic hydroxylated urethane (HEUR).[5,7,22,24,26] When the hydrocarbon end group is connected to the hydrophilic chain by a diurethane spacer, the coupling group becomes part of the hydrophobe. In this paper we investigate SDS interactions with model associative polymers where hydrophobic end groups are directly linked to the PEO chain by ether or ester groups so as to limit the influence of the linker. In this study we have extended the interactions of SDS with fluorinated telechelic AP. Despite the well-known mutual phobicity or antipathy between hydrocarbon and fluorocarbon groups,[27] we have recently reported[3] that the phase and rheological behavior of semifluorinated telechelic PEO were markedly influenced by SDS. The relaxation time (τ) associated with the disengagement of hydrophobic end groups from the aggregate depends on the aggregate core composition. The variation of τ according to the concentration and chemical structure of surfactant was consistent with the formation of mixed aggregates. The present investigations by ^{13}C NMR spectroscopy confirm this assumption and bring information on the environment of SDS inside the hydrophobic core of aggregates in dilute aqueous solutions. Furthermore SANS study allows to determine the aggregation numbers of the different types of aggregates in dilute and semidilute solutions. Combining these techniques, information could be obtained on the structure of the aggregates, their evolution with surfactant concentration and the critical transitions involving a modification of the equilibrium between the different types of aggregates.

2. Experimental Part

2.1. Sample Preparation and Characterization. Telechelic polymers were synthesized by esterification of poly(ethylene glycol) with carboxylic acids in presence of *N*,*N*-dicyclohexylcarbodiimide (DCC) and (dimethylamino)pyridine (DMAP) as described by Hartmann et al.[28] In this way, we obtained functionalized PEO with an ester linker end-capped by hydrogenated groups $C_{17}H_{35}-(PEO)-C_{17}H_{35}$ (denoted $H_{17}-H_{17}$) or semifluorinated ones $C_8F_{17}-C_2H_4-PEO-C_2H_4-C_8F_{17}$ ($F_8H_2-H_2F_8$) and $C_8F_{17}-C_{10}H_{20}-PEO-C_{10}H_{20}-C_8F_{17}$ ($F_8H_{10}-H_{10}F_8$). In order to remove dicyclohexylurea (DCU), byproduct of the reaction, the polymers were purified using molecularly imprinted polymer (MIP) as described elsewhere.[3] Asymmetric end-capped PEO were synthesized by anionic polymerization of ethylene oxide initiated by an alkoxide followed by esterification. These asymmetric polymers contain different hydrophobic end groups: $C_{18}H_{37}-(PEO)-C_2H_4-C_8F_{17}$ ($H_{18}-H_2F_8$), $C_{18}H_{37}-(PEO)-C_{10}H_{20}-C_8F_{17}$ ($H_{18}-H_{10}F_8$). Complete fonctionalization of PEO is controlled by titration of residual hydroxy groups by ^{19}F NMR according to the method previously described[28] (^{19}F NMR spectra of asymmetric polymer ($H_{18}-H_2F_8$) is available as Supporting Information). Molecular weight distribution of polymer was determined by size exclusion chromatography (SEC) using a Shimadzu differential refractometer. To prevent polar interactions between APs and the gel phase, a solution of tetrabutylammonium bromide in tetrahydrofuran (10 mM) is used as eluent (flow rate 1 mL·mn^{-1}). A set of two PLgel columns was used with pore sizes 10^3 and 10^4 Å. A calibration curve was established from poly(ethylene oxide) standards. Asymmetric polymers obtained by anionic polymerization present a narrow distribution with $Ip < 1.1$ (cf. Supporting Information for SEC trace). The polymer samples prepared for this study are described in Table 1.

Poly(ethylene glycol) (Merck) and sodium dodecyl sulfate (Aldrich) were used as received without further purification.

2.2. Tensiometry. Surface tensions were measured with a Lauda tensiometer by the Du Noüy ring method, at 25 °C. Unlike monomeric surfactants, with amphiphilic polymers the system does not go to equilibrium quickly. As a consequence surface tension of AP solutions evolves with time for several hours. In order to obtain coherent results, the equilibrium is considered to be reached after 24 h. In order to minimize the disturbance of the adsorbed interfacial layer, the measuring ring was not detached from the interface between successive measurements. Water used for the preparation of AP solutions was distilled and passed through a Milli-Q (Millipore) ion exchange column.

Table 1. Molecular Characteristics of Hydrophobically Modified PEO

sample	end group	M_w	M_n	I_p
$H_{17}-H_{17}$	$-C_{17}H_{35}$	22400	17000	1.32
$F_8H_2-H_2F_8$	$-(CH_2)_2C_8F_{17}$	19300	16700	1.15
$F_8H_{10}-H_{10}F_8$	$-(CH_2)_{10}C_8F_{17}$	19200	16600	1.16
$H_{18}-H_2F_8$	$-C_{18}H_{37}$ $-(CH_2)_2C_8F_{17}$	23000	21200	1.08
$H_{18}-H_{10}F_8$	$-C_{18}H_{37}$ $-(CH_2)_{10}C_8F_{17}$	19800	18700	1.06

Table 2. Masses, Volumes, and Length Scattering Densities

chemical structure	M (g/mol)	V_i (Å^3)	ρ_i (10^{10} cm^{-2})
$-CH_2\,CH_2\,O$	44	61	0.68
$-COO$	44	73	2.50
$-CH_2$	14	27	−0.31
$-C_8F_{17}$	419	395	3.74
SDS	288	410	0.38
D_2O	20	27	6.40

2.3. ^{13}C NMR Spectroscopy. Proton-decoupled ^{13}C NMR spectra were recorded from D_2O solutions with a Bruker 400 spectrometer operating at 100.6 MHz. All experiments were performed at 25 °C. The sweep width was 23000 Hz, the pulse length 6 μs with a 30° flip angle. The acquisition and delay times were respectively 1.3 and 2 s. Due to the poor abundance of ^{13}C nuclei, in order to obtain a good ratio signal-to-noise, between 4000 and 40000 scans were needed according to SDS concentration. Only carbon signals of SDS and PEO backbone were detected as narrow single lines.

2.4. Small Angle Neutron Scattering (SANS). SANS measurements were carried out at the Laboratoire Léon Brillouin (Saclay, France). The data were collected on beamline PACE at two configurations, one with $\lambda = 7$ Å and a sample-to-detector distance of 1 m, the other with $\lambda = 8$ Å with a sample-to-detector distance of 4.5 m, covering a q range from 0.006 to 0.28 Å^{-1}. The samples were prepared in pure D_2O, and 2 mm light path Hellma quartz cells were used. Empty cell scattering was subtracted and the detector was calibrated with 1 mm H_2O scattering. All measurements were carried out at 25 °C. Data were converted to absolute intensity through a direct beam measurement, and the incoherent background was determined with H_2O/D_2O mixtures. The values of the length scattering densities reported in Table 2 will be used to determine the structure of self-associated aggregates.

3. Results

3.1. Tensiometry. Tensiometry is used extensively to determine the critical micelle concentration (cmc) of surfactants. Surface tension data for $H_{17}-H_{17}$ in pure water are presented in Figure 1. When the polymer concentration rises, the γ value decreases until a plateau. On this plateau the solution interface is saturated by associative polymer so the break point at 5×10^{-5} mol/L (0.1 wt %) marks the critical aggregation concentration (cac) of APs with formation of aggregates in the solution. A comparable critical concentration value (6.8×10^{-5} mol/L) was obtained for hexaethylene glycol *n*-dodecyl ether (6ED), a non ionic surfactant with an ethoxylated segment.[29]

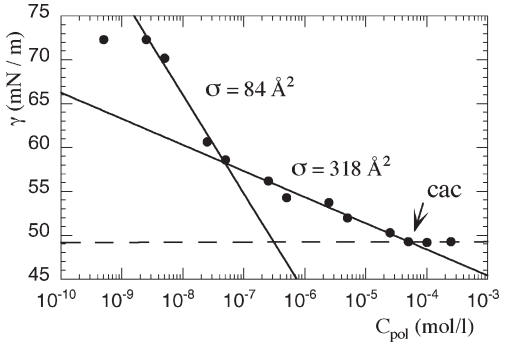

Figure 1. Surface tension of aqueous solution of polymer $H_{17}-H_{17}$ as a function of polymer concentration (C_{pol}) at 25 °C.

An other point of interest to be discussed in this section is the manner in which the surface tension of the binary system decreases with concentration. One can observe a change of slope for $C_{pol} \approx 5 \times 10^{-8}$ mol/L (10^{-4} wt %). From the Gibbs equation (eq 1), it is possible to determine the surface excess quantities (Γ) at the liquid−vapor interface:

$$\Gamma = \frac{-1}{2.3RT}\frac{d\gamma_{LV}}{d(\log C)} \quad (1)$$

$1/\Gamma$ is in relation with the surface area per surfactant molecule (σ)

$$\sigma = \frac{10^{23}n}{\Gamma N} \quad (2)$$

where $n = 1$ for a nonionic surfactant and N is Avogadro's constant. At low polymer concentrations the surface area occupied by one macromolecule $H_{17}-H_{17}$ (σ = 84 Å^2) is comparable with the σ value determined for SDS (σ = 80 Å^2) but larger than that observed with 6ED surfactant (σ = 49 Å^2).[29] In the range of higher AP concentrations σ value is markedly increased (σ = 318 Å^2). These results suggest two types of interfacial adsorption, one involving only one hydrophobic end group per chain with a reduced σ value and the other one involving both end groups with the propensity of the polymer chains to form loops at higher concentrations.

As illustrated in Figure 2, the effect of SDS addition on the surface tension of aqueous 0.2 wt % polymer solutions is different for PEO and $H_{17}-H_{17}$ modified PEO. The interfacial tension of SDS is modified by the presence of PEO in the solution. At low SDS concentrations the lowering of the surface tension is followed by a break in the surface tension curve with a domain of concentration, between 3 and 10 mmol/L, where γ is more or less constant. Finally there is a decrease of γ toward the value obtained in the absence of polymer. The critical concentrations determined by tensiometry, namely, cac = 3 mmol/L, C_2 = 20 mmol/L, and C_m = 40 mmol/L, are in good agreement with previously published measurements.[9,11,13] The critical point C_m is commonly used to describe the concentration when free SDS micelles, without interaction with the PEO chain, begin to form in the solution.

In the presence of hydrophobically modified PEO ($H_{17}-H_{17}$), a steady lowering of γ is observed without plateau level corresponding to cac and C_2 critical concentrations. These results emphasize the specific behavior of hydrophobic end-capped polymer chain. In 0.2 wt % solution, the $H_{17}-H_{17}$ polymer concentration is higher than the cac so the interface is saturated by AP and flowerlike aggregates are formed in the solution. Added SDS molecules can interact with AP end groups within the core of mixed aggregates and replace gradually polymer hydrophobic end-caps at the solution interface. For a SDS concentration of about 30 mmol/L surface tension of the AP solution joins the curve obtained in the absence of polymer. One can consider that the interface is saturated by SDS molecules.

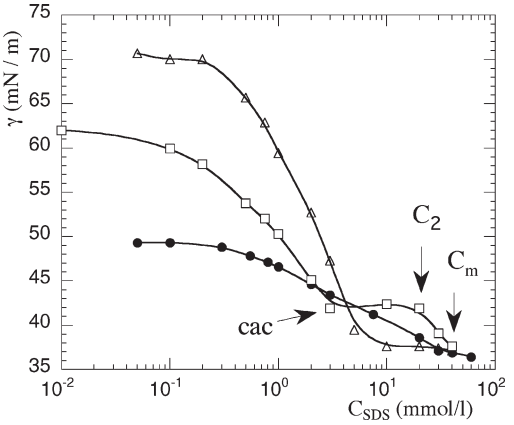

Figure 2. Surface tension as a function of SDS concentration in pure water (Δ) and in presence of PEO (□) or $H_{17}-H_{17}$ (●) 0.2 wt % solutions at 25 °C.

From surface tension measurements, the different types of SDS/AP interactions are deduced indirectly from interfacial behavior. In order to investigate more precisely these interactions, it was necessary to use a sensitive technique for detecting subtle changes of SDS environment in the different aggregated structures.

3.2. ^{13}C NMR Spectroscopy. To investigate the SDS/AP interactions we turned our attention to hydrocarbon ($H_{17}-H_{17}$) and semifluorinated ($F_8H_2-H_2F_8$, $F_8H_{10}-H_{10}F_8$) end-capped PEO. The ^{13}C chemical shift is more sensitive to the environment than proton chemical shift, moreover by ^{13}C NMR all the signals of the various SDS carbons can be resolved. Figure 3 shows the ^{13}C NMR spectrum of an aqueous SDS solution in the presence of 0.2 wt % $H_{17}-H_{17}$, SDS carbon signals were assigned according to previous studies.[11,30] The NMR spectrum presents a well-resolved single line for each carbon atom. Therefore, we conclude that the exchange between the different SDS surrounding states is fast with regard to the NMR time scale.

Let us first consider SDS in aqueous solution. At low concentrations the carbon C_1 chemical shift is independent of SDS concentration up to the cmc (cf. Figure 4). For higher concentrations SDS molecules start to form micelles in equilibrium with free SDS molecules in the solution. In that case, the observed chemical shift δ^{obs} is a weighted average of the two species which evolves linearly with the inverse of concentration:

$$\delta^{obs} = C^{mon}(\delta^{mon} - \delta^{mic})\frac{1}{C} + \delta^{mic} \quad (3)$$

where δ^{mon} represents the chemical shift of free SDS in monomeric state in water, δ^{mic} the chemical shift of SDS involved in a micellar structure, and C^{mon} and C are the monomeric and total SDS concentrations. From eq 3 by extrapolation to 1/C = 0 it is possible to determine the chemical shift of the SDS carbons in a micellar environment, for carbon C_1, δ^{mic} = 69.25 ppm. The chemical shift changes appreciably with the surfactant molecule environment, in a polar aqueous environment δ^{mon} = 69.70 ppm.

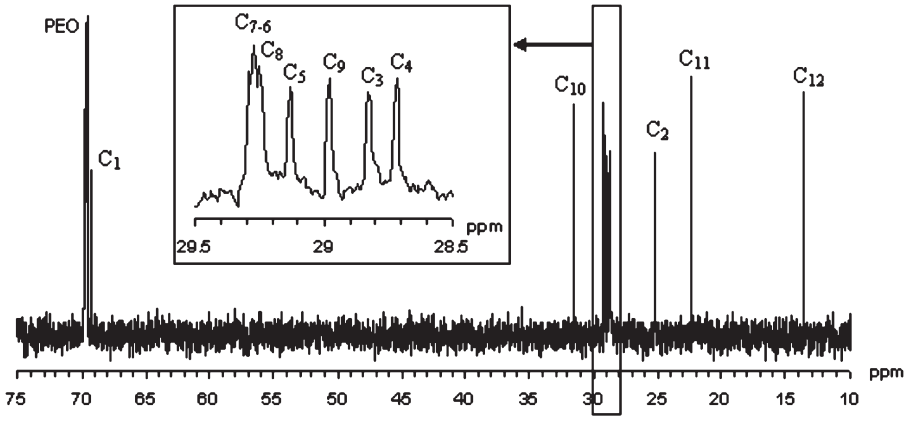

Figure 3. ^{13}C NMR spectrum of aqueous solution of SDS (20 mmol/L) and $H_{17}-H_{17}$ (0.2 wt %). The inset shows the resolution of signals C_3-C_9. Surfactant carbons are numbered starting from the carbon nearest to the ionic head.

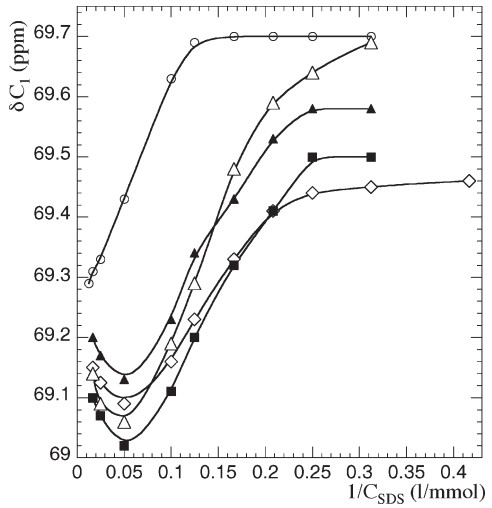

Figure 4. Chemical shift of carbon C_1 as a function of SDS concentration in aqueous solution (o) and in solution at C_{pol} = 0.2 wt % with polymers: PEO (Δ), $H_{17}-H_{17}$ (◇), $F_8H_2-H_2F_8$ (■) or $F_8H_{10}-H_{10}F_8$ (▲), at 25 °C.

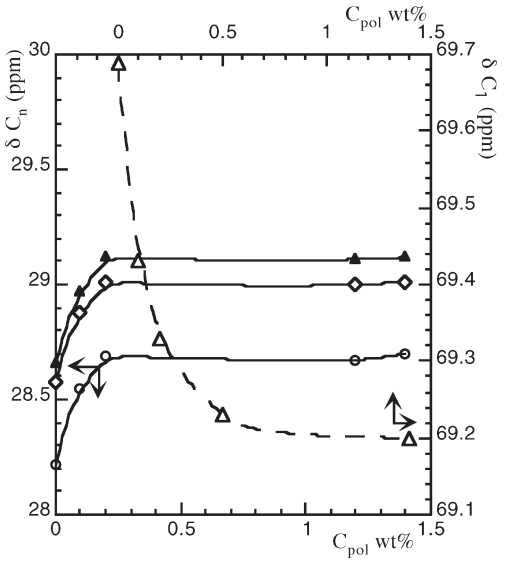

Figure 5. Chemical shift change of the SDS carbons C_1 (Δ), C_3 (○), C_5 (◇), and C_8 (▲) as a function of PEO concentration (C_{pol}) in aqueous solution (C_{SDS} = 8 mmol/L) at 25 °C.

3.2.1. Influence of PEO Concentration. In order to investigate the interactions SDS/PEO, increasing PEO amounts were added to aqueous SDS solution at 8 mmol/L. At this concentration, close to SDS cmc, ^{13}C SDS chemical shifts are equivalent to that observed with SDS monomer in pure water ($\delta^{obs} = \delta^{mon}$). As shown in Figure 5, even at low PEO concentration (C_{PEO} = 0.1 wt %), ^{13}C signals are markedly shifted upfield for carbon C_1 and downfield for the other ones, indicating strong interactions with the polymer chain. A plateau is quickly reached (C_{PEO} = 0.2 wt %) for carbons C_2-C_{12}. The chemical shift $\delta(C_1)$ = 69.2 ppm, observed at higher concentration (C_{PEO} = 1.4 wt %) is equivalent to that determined for SDS in a micellar environment in pure water (δ = 69.25 ppm). This result is entirely coincidental and does not mean that the carbon C_1 SDS environment in micellar aggregates and SDS clusters wrapped by PEO chains are comparable.

From the shift vs shift diagrams of internal carbon pairs (C_3-C_{12}) of the SDS hydrocarbon tail, leading to straight lines, it can be concluded that SDS exchanges between monomeric and aggregated states.[11,31,32] Furthermore the plots shift vs shift for the SDS/PEO/D_2O ternary system are superimposed with the corresponding ones of SDS/D_2O suggesting that the environment of internal carbons (C_3-C_{12}) is comparable in both systems (cf. Figure 6). Thus the carbon C_3-C_{12} chemical shifts of SDS involved in a PEO wrapped aggregate (δ^{wagg}) can be considered to be equivalent to the corresponding chemical shifts of pure surfactant micelles $\delta^{wagg} = \delta^{mic}$.

The shift vs shift diagram of the carbon pair C_1/C_3 deviates from the straight line in presence of PEO and diverges from that for a pure SDS solution (cf. Figure 6) indicating that SDS molecules exchange between at least three states. To clear up the ambiguity with the previous conclusion from the behavior of internal carbons, a transient state is proposed where SDS monomers interact with the polymer chain, in equilibrium with free monomers and aggregates according to Scheme 1.

The monomer SDS binding onto PEO chain was first proposed by Jones.[33] In this state the microenvironment of carbons C_1 and C_2 is different from the one expected for free SDS monomer where SDS polar heads are surrounded by water. On the other hand the local environment of carbons C_3-C_{12} is equivalent in both states 1 and 2, so the observed chemical shift is consistent with an exchange process among two species, monomeric and aggregated SDS. Thus eq 3, transposed to the equilibrium between SDS unimer (free or interacting with PEO) and wrapped aggregates, allows to

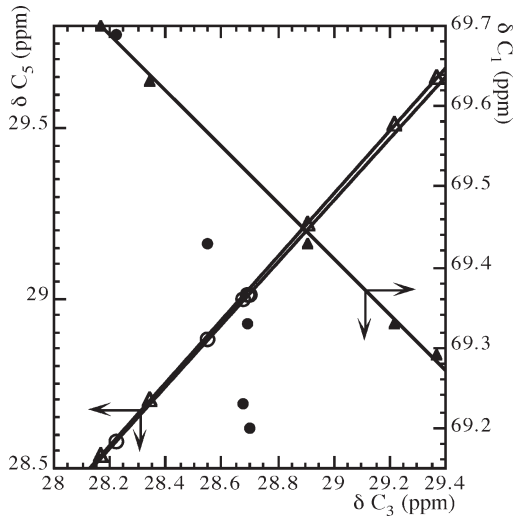

Figure 6. Shift vs shift diagrams of carbons C_5 vs C_3 (open symbols) and carbons C_1 vs C_3 (filled symbols) for SDS solutions in D_2O (Δ) and in the presence of PEO (○). Concerning the PEO/SDS/D_2O ternary system, the SDS concentration is constant (C_{SDS} = 8 mmol/L) and C_{PEO} is ranging between 0.1 and 1.4 wt %.

Scheme 1. Schematic Illustration of SDS/PEO Interactions with the Different States in Equilibrium beyond the cac

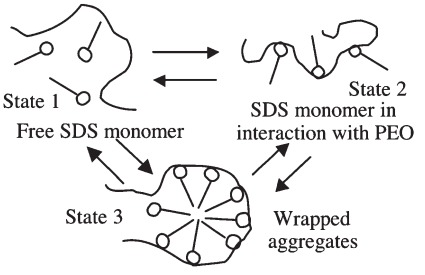

determine an average value of the monomer SDS concentration C^{mon} = 4.8 mmol/L. This critical concentration that can be associated with the cac corresponds to the onset of cooperative binding of SDS aggregates with the PEO polymer chain. Due to the complexation by PEO chain, the SDS aggregation concentration is lowered with respect to the situation in pure water (cac < cmc).

3.2.2. Influence of SDS Concentration. In this study the polymer concentration (C_{pol} = 0.2 wt %) was chosen in order to compare the different ternary systems PEO/SDS/D_2O and AP/SDS/D_2O in a concentration domain (C_{pol} > cac_{AP}) where hydrophobically modified PEO forms aggregates in aqueous solution. At SDS concentrations exceeding 3.2 mmol/L, $\delta(C_1)$ is shifted upfield (cf. Figure 4) indicating the beginning of the aggregation process. The break point corresponding to the cac cannot be clearly determined by straight line fitting. That could be explained by a model involving more than two types of C_1 carbon environment. At higher SDS concentrations (C_{SDS} > 20 mmol/L) $\delta(C_1)$ increases and tends toward δ^{mic} observed in the absence of polymer. This change in chemical shift variation can be explained by the formation of pure SDS micelles without interaction with PEO. The minimum of the curve corresponds to the critical concentration C_m ($C_m \approx 18.5$ mmol/L). Beyond this concentration the PEO chains are saturated by SDS.

The exchange rate between free and SDS associated PEO chain segments is slow with respect to the NMR time scale. The NMR experiment can distinguish the sharp signal

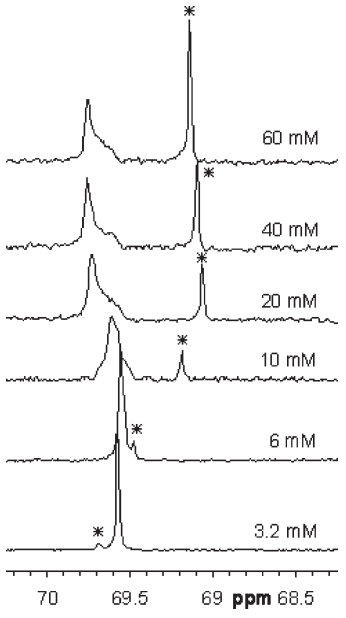

Figure 7. Influence of SDS concentration on the ^{13}C NMR spectra corresponding to $-CH_2$ groups of PEO at C_{PEO} = 0.2 wt %: (∗) signal of carbon C_1.

at δ = 69.58 ppm due to free PEO chain at low SDS concentration. As shown in Figure 7, when SDS concentration increases the signal is broadened and shifted downfield with the appearance of a peak at δ = 69.75 ppm corresponding to PEO chain wrapped around SDS aggregates. The broad signal observed at higher concentration indicates that the aggregation process does not involve only one type of SDS/PEO interaction with a well-defined structural complex. A similar evolution of the resonance of $-CH_2$ groups of the polymer chain as a function of SDS concentration is observed for end-capped PEO (cf. data presented below).

3.2.3. Influence of Associative Polymer $H_{17}-H_{17}$. Figure 4 compares the dependence of carbon C_1 chemical shift on SDS concentrations in the presence of 0.2 wt % PEO and $H_{17}-H_{17}$ end-capped PEO. At SDS concentrations lower than 4 mmol/L, the $\delta(C_1)$ values are markedly decreased in the presence of AP. This is due to the presence of hydrophobic $C_{17}H_{35}$ alkyl end groups that allows the formation of mixed aggregates with the insertion of surfactant molecules into the core of flowerlike aggregates. The evolution of the chemical shifts of the different carbon atoms with the SDS concentration can be explained by an increasing participation of SDS in mixed aggregates. This process supposes that the composition of mixed aggregates evolves with SDS concentration. If we consider an equilibrium between free SDS monomer and SDS involved in mixed aggregates, the onset concentration for the uncooperative binding (C_{UB}) between SDS molecules and the hydrophobic end groups of AP can be evaluated. This critical concentration was found to be much lower than the cac and possesses a value ranging between 0.8 and 1 mmol/L according to the SDS C_3-C_{12} carbon considered. This value is consistent with previous results obtained by Dai et al.[22] ($C_{UB} \approx 0.4$ mmol/L) for HEUR-C12 system.

With increasing SDS concentration, the deviation of the $\delta(C)$ curves is attributed to the onset of cooperative binding between AP chains and SDS. The critical concentration ($C_{SDS} \approx 4$ mmol/L) for such binding is comparable to the cac observed in the presence of PEO. However, beyond the cac, the binding mechanism of AP/SDS system is different from that of PEO/SDS. By analogy with the PEO/SDS

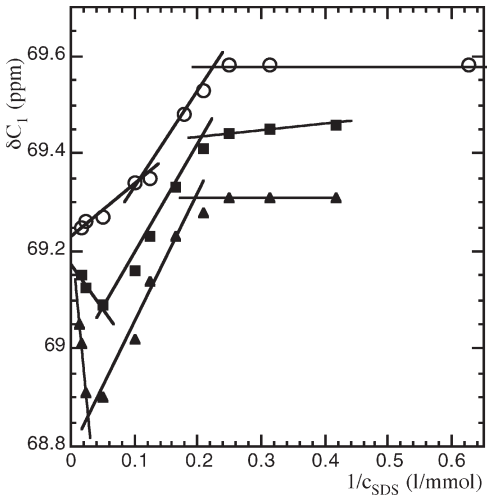

Figure 8. Chemical shift of carbon C_1 as a function of reciprocal SDS concentration in D_2O with different $H_{17}-H_{17}$ concentrations: 0.1 wt % (○) 0.2 wt % (■), and 0.5 wt % (▲).

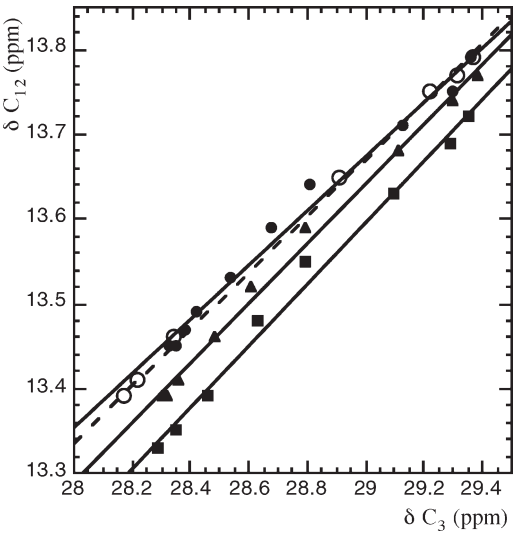

Figure 9. Relationship between $\delta(C_{12})$ and $\delta(C_3)$ for SDS solutions in D_2O (*o*) (dotted line) and in 0.2 wt % AP solutions (solid line) with hydrocarbon end groups $C_{17}H_{35}$ (●) and semifluorinated ones $C_8F_{17}-(CH_2)_{10}$ (▲) or $C_8F_{17}-(CH_2)_2$ (■).

system it was suggested[9a] the formation of SDS micelles wrapped by the loops of flowerlike AP aggregates. This assumption is not coherent with SANS results that will be developed further. From SANS experiments it was clearly shown that aggregates, in this domain of SDS concentrations ($C_{SDS} > 4$ mmol/L), are mainly constituted by SDS molecules with a few number of AP chains. Thus the cooperative binding transition, in the presence of AP, could be explained by the change from polymer induced mixed aggregates to SDS induced micellar aggregates. In the former state ($C_{SDS} <$ cac), SDS molecules fit into pre-existing flowerlike aggregates while in the latter one, SDS micelles with a few alkyl end groups are complexed by the AP chains.

When the SDS concentration reaches the critical concentration C_m ($C_m = 18.5$ mmol/L) the behavior of $H_{17}-H_{17}$/SDS system is similar to that of PEO/SDS. In the domain of concentrations $C_{SDS} > C_m$, the chemical shifts are comparable for both systems. Beyond the concentration C_m, the polymer chains are saturated, and free SDS micelles are formed.

Carbons C_1 and carbon C_2 to a less extent, are more sensitive to the local environment of SDS polar head. The nonlinearity of the shift vs shift plots (cf. Supporting Information) confirms that the aggregation process does not involve just the monomer and a well-defined aggregated structure. Linear regression of the different part of the plot $\delta(C_1)$ vs $1/C_{SDS}$ allows to determine the critical concentrations cac and C_m with different AP concentrations. The cac values, slightly increasing from 4.1 mmol/L up to 4.8 mmol/L, are not directly proportional to polymer concentration increase. The transition from mixed aggregates to micellar aggregates is mainly determined by the SDS concentration. On the other hand the critical concentration C_m, which corresponds to the saturation of polymer chain by SDS, is more dependent on AP concentration (cf. Figure 8). With increasing polymer concentration, more SDS molecules are required to saturate the PEO polymer chains (cf. Table 3).

The shift vs shift diagrams of C_3-C_{11} carbons (cf. Supporting Information) lead to straight lines and superimpose with the corresponding ones of SDS/D_2O system suggesting that the microenvironment of SDS internal carbons in the core of mixed aggregates or micellar aggregates is not modified by the presence of AP alkyl end groups. Nevertheless, the $\delta(C_{12})$ vs $\delta(C_3)$ plot (cf. Figure 9) reveals that the microenvironment of SDS terminal carbon C_{12} is slightly modified by the presence of AP end group.

3.2.4. Influence of Associative Polymer End Group. Figure 4 shows the carbon C_1 chemical shift as a function of $1/C_{SDS}$ for different APs end-capped by hydrogenated end groups ($H_{17}-H_{17}$) or semifluorinated ones ($F_8H_2-H_2F_8$ and $F_8H_{10}-H_{10}F_8$). At lower SDS concentrations $\delta(C_1)$ is markedly affected by the chemical structure of AP end groups. In this concentration range, the very slight variation of $\delta(C_1)$ vs $1/C_{SDS}$ does not allow an accurate determination of C_{UB} with fluorinated APs. The uncooperative binding occurs probably at very low SDS concentration ($C_{SDS} < 0.1$ mmol/L) in agreement with previously reported phase behavior of strongly associated fluoropolymers.[3] Homogeneous phase of $F_8H_{10}-H_{10}F_8$/SDS/H_2O ternary system was obtained with a minimal SDS concentration of about 2.10^{-2} mmol/L.

The observed chemical shift is a weighted average of the different species involved in the equilibrium and does not reflect directly the microenvironment of the SDS carbon in mixed aggregates. Nevertheless the $\delta(C_1)$ evolution with AP chemical structure proves that SDS molecules are involved in the core of mixed aggregates thereby reflecting a certain compatibilty between the hydrocarbon SDS tail and the semifluorinated end groups. To determine more precisely the effect of AP end groups on the structure and composition of the core of mixed aggregates we examined the local environment of internal carbons by the shift vs shift diagram. The farther the atom from the polar headgroup, the larger the change of chemical shift compared with SDS/D_2O system. Thus, the end of the SDS hydrophobic tail should be more sensitive to the environment in mixed aggregates. The plot shift vs shift of the carbon pair C_{12}/C_3 is reported in Figure 9 for SDS in pure D_2O and for the AP/SDS/D_2O ternary systems. The linear relationship observed over the SDS concentration range for the different systems is consistent with an equilibrium involving two main species, mixed aggregates and SDS micellar aggregates. These results suggest that the local environment of the carbons of the SDS hydrocarbon tail in wrapped aggregates is very similar to the free micelle one.

For the $H_{17}-H_{17}$/SDS/D_2O system, the shift vs shift plot is superimposed with the corresponding one of the SDS/D_2O system. Thus the presence of hydrocarbon end group does

Table 3. Parameters Obtained from ^{13}C NMR Data

sample	C_{pol} (wt %)	cac or cmc[a] (mmol/L)	C_m[a] (mmol/L)
SDS		8.1	
SDS + PEO	0.2	4.8[b]	18.5
SDS + $H_{17}-H_{17}$	0.1	4.1	8.7
SDS + $H_{17}-H_{17}$	0.2	4.5	18.5
SDS + $H_{17}-H_{17}$	0.5	4.8	34.3
SDS + $F_8H_{10}-H_{10}F_8$	0.2	4.4	18.9
SDS + $F_8H_2-H_2F_8$	0.2	4.1	18.4

[a] Values obtained by linear regression of C_1 carbon chemical shift, margin of error ± 0.2 mmol/L. [b] Average value determined from internal carbons (C_3-C_{12}) chemical shifts.

not modify the microenvironment of SDS tail. On the contrary, due to the presence of perfluorinated segment, the $\delta(C_{12})$ vs $\delta(C_3)$ plot is moved. The shift is more pronounced in presence of the highly fluorinated $C_8F_{17}-(CH_2)_2$ end group, thus confirming the formation of mixed aggregates between SDS and fluorinated end-capped PEO. At constant polymer concentration (C_{pol} = 0.2 wt %), the critical concentrations cac and C_m determined from $\delta(C_1)$ data are independent of the chemical structure of AP hydrophobic end groups (cf. Table 3). These findings for cac values are consistent with the onset of cooperative binding between SDS and AP and the formation of SDS induced micellar aggregates. Therefore the transition between mixed and micellar aggregates is governed by the SDS concentration independently of hydrophobic end-cap structure. The formation of micellar aggregates, mainly constituted by SDS molecules, depends on the PEO chain capability to complex and stabilize aggregates with a lower aggregation number than that observed in pure water.

^{13}C NMR spectra of $-OCH_2-$ groups of the polymer chain in $F_8H_{10}-H_{10}F_8$/SDS/D_2O system are shown in Figure 10. At low SDS concentration the spectrum exhibits the sharp signal (δ = 69.58 ppm) corresponding to the free polymer chain. Increasing surfactant concentration, a second signal appears and moves downfield up to δ = 69.81 ppm. At C_{SDS} = 10 mmol/L, the coexistence of two main peaks shows that the polymer chain exchange slowly between free and aggregated states. The broadened signals observed at higher SDS concentrations reveal the presence of various environments for carbon C_1 corresponding to different states of SDS/polymer chain interactions which exchange slowly. The SANS study will give more information about the structure and composition of the aggregated species.

3.3. Small Angle Neuton Scattering (SANS). Aqueous solutions of AP were prepared in D_2O to enhance the scattering contrast at concentrations ranging between 0.5 and 5 wt %. For monodisperse assemblies of spherically symmetric colloidal particles, the scattering intensity can be expressed by

$$I(q) = \Phi V_0 (\Delta\rho)^2 P(q) S(q) \quad (4)$$

where q is the wave vector, Φ is the aggregate volume fraction, V_0 is the dry volume of an aggregate, and $\Delta\rho$ is the contrast (i.e., the difference in the scattering-length density between the dry aggregate and the solvent, D_2O). $P(q)$ is the form factor and $S(q)$ is the structure factor that expresses the interaction between aggregates. Figure 11 displays the neutron scattering intensity obtained for $H_{17}-H_{17}$ AP in dilute regime (C_{pol} = 0.5 and 1 wt %). The intensities displayed in Figure 11 bring information on form factors of noninteracting self-assembled aggregates. For

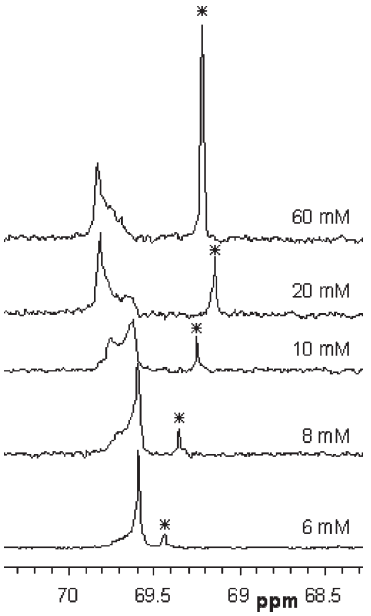

Figure 10. Influence of SDS concentration on the ^{13}C NMR spectra corresponding to $-CH_2$ groups of the polymer chain of $F_8H_{10}-H_{10}F_8$ at C_{Pol} = 0.2 wt %: (*) signal of carbon C_1.

$H_{17}-H_{17}$/SDS/D_2O ternary system, the asymptotic scattering functions at low wave vector q are well reproduced by a Guinier approximation according to eq 5:

$$I(q) = I_0 \exp\left(\frac{-q^2 {R_G}^2}{3}\right) = \Phi V_0 \Delta\rho^2 \exp\left(\frac{-q^2 {R_G}^2}{3}\right) \quad (5)$$

In the Guinier regime, eq 5 accounts for the overall size of the aggregate and allows to determine its radius of gyration R_G. In the dilute regime ($q \rightarrow 0$) the decrease of I_0 observed in presence of SDS means that the mass of mixed micellar aggregates is reduced with regard to the one of an AP aggregate. The radius of gyration of $H_{17}-H_{17}$ flowerlike aggregates can be estimated from the change in slope at $q \approx 0.025$ Å^{-1}, leading to R_G = 78 Å. The difference of scattered intensities between ternary mixture $H_{17}-H_{17}$/SDS/D_2O and the corresponding binary systems, at low q values, reveals strong AP/SDS interactions and consequently modifications of the structure and size of self-assembled species. The aggregation number (p) of the flowerlike aggregates can be determined from the extrapolated scattered intensity at $q \rightarrow 0$, $I_0 = V_0 \Phi \Delta\rho^2$ The excess scattering length densities ($\Delta\rho$) of the aggregate with respect to D_2O were calculated from data established by Sears[34] (cf. Table 2). The total aggregation number determined from the prefactor of the exponential in eq 5 can be expressed by: $p = \frac{V_0}{V_{0_{SDS}} p_{SDS}/p + V_{0_{AP}} p_{AP}/p}$ where $V_{0_{SDS}}$ and $V_{0_{AP}}$ are the dry volumes of SDS and associative polymer, respectively, and p_{SDS} and p_{AP} are the partial aggregation numbers of SDS and AP. If we suppose an uniform and homogeneous distribution of SDS and AP between aggregates, the ratios p_{SDS}/p and p_{AP}/p can be determined from initial conditions. The aggregate sizes and aggregation numbers of the different self-associated species are reported in Table 4. The increased mass of mixed aggregates upon addition of AP and the decreased radius of gyration of flowerlike AP aggregates in presence of SDS confirm ^{13}C NMR findings with the formation of a new type of aggregate in this range of concentrations ($C_{pol} < C^*$, cac < $C_{SDS} < C_m$), called "micellar aggregates". As shown by the values of

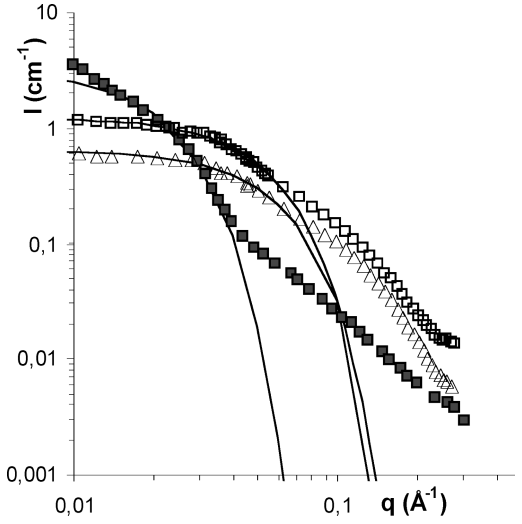

Figure 11. Neutron scattered intensities from dilute aqueous solutions of telechelic polymer $H_{17}-H_{17}$ in presence of SDS (8 mmol/L) at C_{pol} = 0.5 wt % (△) and 1 wt % (□) and AP alone (without SDS) at C_{pol} = 0.5 wt % (■). The solid lines are asymptotic behavior derived from eq 5.

Table 4. Structural Parameters of Self-Assembled Aggregates Involving SDS and/or Associative Polymer $H_{17}-H_{17}$ in Dilute and Semidilute Solution[a]

C_{SDS} (mmol/L)	C_{pol} (wt %)	R_G (Å)	p_{AP}	p_{SDS}	D (Å)
16	0	16 ± 1		66	
0	0.5	78 ± 1	7		
8	0.5	30 ± 1	0.7	23	
8	1.0	33 ± 1	1.0	15	
8	3.0		8.0	45	210 ± 8
8	5.0		9.0	30	185 ± 6

[a] D is the most probable distance between aggregates as deduced from the location of the scattering peak.

aggregation numbers, the micellar aggregates are formed mainly by SDS molecules with a few APs. The formation of these aggregates is governed by SDS. As suggested by Abrahmsén et al.,[35] SDS micelles act as seed for the associative polymer aggregation.

The SDS aggregation number (p_{SDS}) at C_{SDS} > cac is lower than that of free SDS micelles in water. Furthermore in dilute regime, p_{SDS} evolves with polymer concentration, the larger the polymer concentration, the smaller the aggregation number. Our findings ($15 \le p_{SDS} < 25$) are consistent with results reported by Zana et al.[17] for PEO/SDS system. The average p_{AP} value is equal or less than 1, meaning that the polymer chain is long enough to participate on average in two aggregates as obtained by Bernazzani et al.[11] with unmodified PEO. At constant SDS concentration (C_{SDS} = 8 mmol/L), with increasing AP concentration, the structure and composition of micellar aggregates are modified. This is a main difference with AP aggregation behavior. When expressed in terms of $I(q)/\Phi$, the neutron intensities of the binary system (AP/D_2O) are found to superimpose in the high q range,[36] whatever the polymer concentration ranging from 0.5 to 8 wt % indicating that the aggregate local structure remains unchanged. On the contrary in the ternary system ($H_{17}-H_{17}/SDS/D_2O$), the scattering curves in the high q range evolve as a function of AP concentration (cf. Figure 12). Due to the presence of SDS, the qualitative changes in scattering reflect modifications of aggregates in form and composition according to the ratio AP/SDS.

In the semidilute regime ($C_{AP} > C^*$), the structure factor $S(q)$ affects intensities in the low q range and a correlation

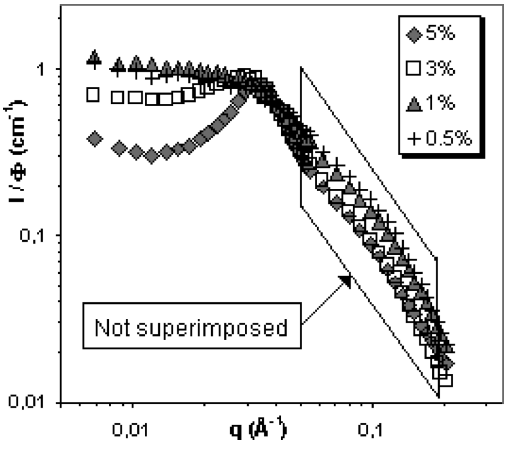

Figure 12. Neutron scattered intensity normalized by the aggregate volume fraction Φ from aqueous solutions of telechelic polymer $H_{17}-H_{17}$ for C_{AP} = 0.5, 1, 3, and 5 wt %, with SDS (8 mmol/L). In the high q range, the various spectra according to polymer concentrations do not superimpose as observed for binary system ($AP-D_2O$).[36]

Table 5. Structural Parameters of Self-Assembled Aggregates Involving SDS (C_{SDS} = 8 mmol/L) and Various Associative Polymers in Aqueous Semidilute Solution (C_{AP} = 3 wt %)

polymer	V_{eg}* (Å^3)[a]	p_{AP}	p_{SDS}	D (Å)
$H_{17}-H_{17}$	532	8 ± 1	45 ± 5	210 ± 8
$F_8H_2-H_2F_8$	522	9 ± 1	47 ± 7	215 ± 8
$F_8H_{10}-H_{10}F_8$	765	16 ± 2	85 ± 10	260 ± 10
$H_{18}-H_{10}F_8$		12 ± 2	68 ± 8	240 ± 10
$H_{18}-H_2F_8$		7 ± 1	40 ± 5	200 ± 10

[a] V_{eg}* is the end group molecular volume. For SDS, V_{eg} = 410 Å^3.

peak appears at q_{max} = 0.03 and 0.034 Å^{-1}, respectively for 3 and 5 wt % solutions. The structure factor $S(q)$ is due to electrostatic repulsive interactions between aggregates. The wave vector q_{max} of the peak position is related to the ordering of the aggregates and provides information on the average interaggregate distance D. The typical nearest neighbor distance D can be determined from $q_{max} = 2\pi/D$. Assuming that aggregates adopt a regular organization in space on a simple cubic lattice instead of taking their true liquidlike order, the aggregation number p can be estimated from the aggregate density N/V and AP molar concentration C, $p = CN(V/N)$. (According to the previous hypothesis, the unit cell contains one aggregate $V/N = D^3$.) The aggregation numbers p_{SDS} and p_{AP} are significantly increased above the threshold concentration C^* corresponding to the sol−viscoelastic transition with the formation of a multiconnected network of aggregates. Above C^*, the micellar aggregates defined in the dilute regime do not exist any longer and are replaced by mixed aggregates. As was observed in the dilute regime, the SDS aggregation number of mixed aggregates decreases when the AP concentration increases.

At constant concentrations (C_{AP} = 3 wt %, C_{SDS} = 8 mmol/L), scattered intensities from semidilute solutions are slightly affected by the chemical structure of telechelic polymer end group and by the polymer architecture (symmetric or asymmetric). The aggregate size and the average interaggregate distance D mainly depend on the hydrophobic end group volume (cf. Table 5) and incidentally on chemical nature (fluorinated or hydrocarbon group). Independtly of the compatibility between fluorinated end groups and SDS hydrocarbon chain, mixed aggregates are formed, and the larger the hydrophobic end group, the higher the aggregation numbers. In the absence of surfactant, a similar conclusion was reported by Tae et al.[37] with fluorinated HEUR from

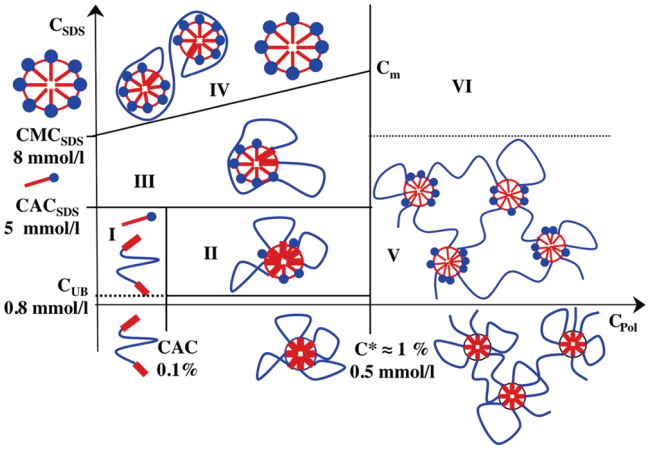

Figure 13. Schematic overview of aggregate structures as a function of telechelic AP and SDS concentrations.

SANS experiments. These authors demonstrated that the hydrophobic length of semifluorinated end groups governs the aggregation number. The aggregate mass of asymmetric telechelic polymers seems to be equivalent or intermediate between the homologous symmetric telechelic polymer ones.

4. Discussion

From experimental findings obtained by tensiometry, ^{13}C NMR spectroscopy and SANS, the interactions between SDS and telechelic associative polymers can be elucidated. They are described in a schematic diagram (cf. Figure 13). These analytical techniques bring specific information concerning critical transitions between different types of SDS/telechelic polymer self-association and allow to define the structure and composition of the aggregates. The diagram provides a useful tool to describe the evolution of the aggregation process according to the concentrations of surfactant and telechelic polymer. In domain I the interactions between SDS and AP in a monomeric state are limited, concentrations are too low to engage in the aggregation process. Above a certain critical concentration (cac) determined by tensiometry, self-assembled aggregates of telechelic polymers are formed. The aggregation number (p_{AP} = 7) in the binary system $H_{17}-H_{17}$/water was determined by SANS. As conjectured by Semenov et al.,[2] it was found, based on SANS experiments,[36] that telechelic associative polymers self-assemble into flowerlike aggregates.

Domain II describes the behavior of AP aggregates in presence of SDS and the formation of mixed aggregates. The uncooperative binding occurring between SDS and hydrophobic polymer end group was detected by Dai et al.[22] with SDS/HEUR. This process driven by telechelic polymer association is operative at low SDS concentrations. The critical concentration of uncooperative binding (C_{UB}) of $H_{17}-H_{17}$/SDS/D_2O system, estimated by ^{13}C NMR spectroscopy, is well below the SDS cac ($C_{UB} \approx 1$ mmol/L). The variation in SDS carbon chemical shifts according to the AP hydrophobic end group reveals a modification of the SDS tail local environment and produces further evidence of the formation of mixed aggegates.

In dilute regime ($C_{AP} < C^*$), when the SDS concentration reaches the cac (domain III), a cooperative binding between SDS and PEO chain occurs. Beyond this transition, clearly shown by ^{13}C NMR spectroscopy, mixed micelles reorganize into a necklacelike conformation where PEO chains wrapped around micellar aggregates. The SDS aggregation number determined from SANS experiment remains lower than that observed with SDS in pure water. With a limited AP aggregation number ($p_{AP} \approx 1$), the micellar aggregate structure is different from the flowerlike aggregate one. That could be explained by the complexation of the aggregate core by PEO chain. ^{13}C NMR spectra of $-OCH_2-$ groups of PEO chain exhibit a sharp signal at low SDS concentrations due to free PEO chains in the aqueous environment. Increasing SDS concentration leads to the emergence and development of a signal downfield attributed to PEO segments in close interaction with SDS aggregates. With the onset of cooperative binding, the cac corresponds to a transition between an associative polymer driven process and a surfactant driven process.

With a further increase in SDS concentration, the critical concentration C_m is reached with the formation of free SDS micelles (cf. Figure 13, domain IV). The equilibrium between micellar aggregates and free SDS micelles is clearly shown by ^{13}C NMR results. The critical concentration C_m corresponds to the saturation of polymer chains by SDS and depends on polymer concentration.

In the semidilute regime (domain V), at polymer concentrations beyond C^*, the investigation of aggregate structure was limited to the SANS technique. In a previous paper,[6] we have related the influence of SDS on the rheological behavior of telechelic polymers in aqueous medium at $C_{pol} > C^*$. To explain the augmentations of the elastic plateau modulus (G_0) and relaxation time (τ) in presence of SDS, it was suggested the formation of mixed aggregates with SDS molecules incorporated into the core of flowerlike micelles. The viscoelastic response of semidilute solution in presence of different surfactants (hydrogenated or fluorinated) was correlated with the interactions between hydrophobic end groups and surfactant inside mixed aggregates.[3] SANS results reported in the present paper confirm these assumptions and prove the formation of mixed aggregates. The polymer aggregation numbers, determined by SANS, remain practically unchanged ($p_{AP} \approx 8$) in comparison with those observed in the binary system (without surfactant p_{AP} = 7). While the SDS aggregation number is significantly increased ($p_{SDS} > 30$) when compared to aggregates in dilute regime. In the semidilute regime the structure of mixed aggregates and bridging between aggregates leading to the transient network as observed in the rheological response[3] are driven by the associative polymer. The peak of scattering intensity related to structure factor accounts for the interactions between aggregates.

The semidilute regime beyond a SDS concentration C_{SDS} = 8 mmol/L (domain VI) was not investigated, for the moment. It has been shown by Zhang et al.[5] that an excess of SDS (about 33 SDS per AP hydrophobe) leads to the network break-up. The evolution of the network topology will be associated with a gradual change of aggregate structure. The values of p_{SDS} that increase with the ratio SDS/AP necessary reach a maximum compatible with the mixed aggregate structure. At the same time a decrease of the polymer aggregation number (p_{AP}) could explain the reduction of viscosity in relation with a reduced density of elastically active chains and a limited functionnality of aggregates. Critical concentration analogous to the cac observed in dilute regime leading to the formation of micellar aggregates cannot be completely ruled out. More specific investigations, out of the scope of this study, are needed to determine the aggregate structures and possible transitions between different states.

Without surfactant, the inner structure of flowerlike aggregates in the binary system AP/water remains unchanged in a large range of concentration including dilute and semidilute regime.[36] Due to the presence of surfactant, present results show that the behavior and the structure of AP aggregates are strongly modified and depend on the concentrations of associative polymer and surfactant. Inside the various domains corresponding to different types of associations and interactions, the inner structure of self-assembled aggregates evolves with SDS/AP ratio.

5. Conclusion

In this paper, the interactions between SDS and associative polymers in aqueous solution were investigated by ^{13}C NMR using the SDS hydrocarbon tail as an internal probe. In this way, it is possible to establish the SDS environment (free monomer, free micelle, aggregates with hydrophobic polymer end groups) and the equilibrium between the different species. Two types of aggregates were clearly identified, micellar aggregates and mixed aggregates whose formation is governed, respectively, by surfactant and the associative polymer. In the dilute regime, three SDS critical concentrations are determined. With increasing SDS concentration, the first one corresponds to uncooperative binding (C_{UB}) between SDS and AP flowerlike aggregates leading to the formation of mixed aggregates. The critical aggregation concentration (cac) determines the onset of cooperative binding with the formation of micellar aggregates. Beyond the saturation concentration (C_m), free SDS micelles are formed. Despite the well-known poor affinity between hydrocarbon and fluorocarbon groups, the formation of mixed aggregates involving SDS and polymer fluorinated end-caps was clearly shown.

From neutron scattering studies it was possible to estimate the aggregation number of SDS (p_{SDS}) and associative polymer (p_{AP}) in the hydrophobic core of surfactant micelles and mixed aggregates. In dilute regime, the strong interactions between anionic surfactant and PEO bring about a decrease of the SDS aggregation number ($p_{SDS} \approx 20$ in micellar aggregates) as well as a decrease of the size of the flowerlike aggregates. The evolution of aggregate structure with polymer concentration is shown by change of the normalized neutron scattered intensity at large wave vectors. In semidilute regime, mass and volume of mixed aggregates increase with the volume of the associative polymer end group.

A combined study by ^{13}C NMR spectroscopy and SANS of this intriguing system reveals that self-assembled species are in constant evolution according to the ratio SDS/AP.

Supporting Information Available: AP characterization via figures showing an SEC trace, ^{19}F NMR spectra and titration of residual OH, and ^{13}C NMR shift vs shift diagrams of SDS involved in different systems: SDS/D_2O and associative polymer/SDS/D_2O. This material is available free of charge via the Internet at http://pubs.acs.org.

References and Notes

(1) Winnik, M.; Yekta, A. *Curr. Opin. Colloid Interface Sci.* **1997**, *4*, 424–436.
(2) Semenov, A. N.; Joanny, J. F.; Khokhlov, A. R. *Macromolecules* **1995**, *28*, 1066–1075.
(3) Rufier, C.; Collet, A.; Viguier, M.; Oberdisse, J.; Mora, S. *Macromolecules* **2008**, *41*, 5854–5862.
(4) Amis, E. J.; Hu, N.; Seery, T. A. P.; Hogen-Esch, T. E.; Yassini, M.; Hwang, F. In *Hydrophilic Polymers: Performance with Environmental Acceptability*; Glass, J. E., Ed.; ACS Advances in Chemistry Series 248; American Chemical Society: Washington, DC, 1996; Chapter 16.
(5) Zhang, K.; Xu, B.; Winnik, M. A.; Macdonald, P. M. *J. Phys. Chem.* **1996**, *100*, 9834–9841.
(6) Calvet, D.; Collet, A.; Viguier, M.; Berret, J.-F.; Séréro, Y. *Macromolecules* **2003**, *36*, 449–457.
(7) Annable, T.; Buscall, R.; Ettelaie, R.; Shepherd, P.; Wittlestone, D. *Langmuir* **1994**, *10*, 1060–1070.
(8) Cooke, D. J.; Dong, C. C.; Lu, J. R.; Wang, Y.; Han, B.; Yan, H.; Thomas, R. K. *Langmuir* **1998**, *14*, 6054–608.
(9) (a) Dai, S.; Tam, K. C. *J. Phys. Chem. B* **2001**, *105*, 10759–10763. (b) *Colloids Surf. A: Physicochem. Eng. Asp.* **2006**, *289*, 200-206.
(10) (a) Olofsson, G.; Wang, G. *Pure Appl. Chem.* **1994**, *66*, 527–532. (b) Wang, G.; Olofsson, G. *J. Phys. Chem. B* **1998**, *102*, 9276–9283.
(11) Bernazzani, L.; Borsacchi, S.; Catalano, D.; Gianni, P.; Mollica, V.; Vitelli, M.; Asaro, F.; Feruglio, L. *J. Phys. Chem. B* **2004**, *108*, 8960–8969.
(12) Wang, Y.; Han, B.; Yan, H.; Cooke, D. J.; Lu, J.; Thomas, R. K. *Langmuir* **1998**, *14*, 6054–6058.
(13) Frohner, S. J.; Belarmino, A.; Zanette, D. *Colloids Surf. A: Physicochem. Eng. Asp.* **1998**, *137*, 131–139.
(14) Gjerde, M. I.; Nerdal, W.; Hoiland, H. *J. Colloid Interface Sci.* **1998**, *197*, 191–197.
(15) Brown, W.; Fundin, J.; Miguel, M. G. *Macromolecules* **1992**, *25*, 7192–7198.
(16) Cabane, B.; Duplessix, R. *J. Phys. (Paris)* **1982**, *43*, 1529–1542.
(17) Zana, R.; Lianos, P.; Lang, J. *J. Phys. Chem.* **1985**, *89*, 41–44.
(18) Maltesh, C.; Somasundaran, P. *Langmuir* **1992**, *8*, 1926–1930.
(19) di Meglio, J.-M.; Baglioni, P. *J. Phys. Chem.* **1994**, *98*, 5478–5480.
(20) Wang, Y.; Lu, D.; Yan, H.; Thomas, R. K. *J. Phys. Chem.* **1997**, *101*, 3953–3956.
(21) Cao, M.; Hai, M. *J. Chem. Eng. Data* **2006**, *51*, 1576–1581.
(22) Dai, S.; Tam, K. C.; Wyn-Jones, E.; Jenkins, R. D. *J. Phys. Chem. B* **2004**, *108*, 4979–4988.
(23) Hu, Y.-Z.; Zhao, C.-L.; Winnik, M. A.; Sundararajan, P. R. *Langmuir* **1990**, *6*, 880–883.
(24) Dai, S.; Tam, K. C.; Jenkins, R. D. *J. Phys. Chem. B* **2001**, *105*, 10189–10196.
(25) Haldar, B.; Chakrabarty, A.; Mallick, A.; Mandal, M. C.; Das, P.; Chattopadhyay, N. *Langmuir* **2006**, *22*, 3514–3520.
(26) Dai, S.; Tam, K. C.; Jenkins, R. D. *Macromolecules* **2001**, *34*, 4673–4675.
(27) Dunitz, J. D. *ChemBioChem* **2004**, *5*, 614–621.
(28) Hartmann, P.; Collet, A.; Viguier, M. *J. Fluor. Chem.* **1999**, *95*, 145–151.
(29) Suzuki, T.; Ueno, M.; Meguro, K. *J. Am. Oil Chem. Soc.* **1981**, 800–803.
(30) Cabane, B. *J. Phys. Chem.* **1977**, *81*, 36–42.
(31) Leibfritz, D.; Haupt, H.; Dubischar, N.; Lachmann, H.; Oekonomopulos, R.; Jung, G. *Tetrahedron* **1982**, *38*, 2165–2181.
(32) Polster, J.; Lachmann, H. *Spectrometric Titrations*; VCH: Weinheim, Germany, 1989; Chapter 18.
(33) Jones, M. N. *J. Colloid Interface Sci.* **1967**, *23*, 36–42.
(34) Sears, V. F. *Neutron News* **1992**, *3*, 26–36.
(35) Abrahmsén-Alami, S.; Stilbs, P. *J. Phys. Chem.* **1994**, *98*, 6359–6367.
(36) Séréro, Y.; Aznar, R.; Porte, G.; Berret, J.-F.; Calvet, D.; Collet, A.; Viguier, M. *Phys. Rev. Lett.* **1998**, *81*, 5584–5587.
(37) Tae, G.; Kornfield, J. A.; Hubbell, J. A.; Lal, J. *Macromolecules* **2002**, *35*, 4448–4457.